Invited Paper

Terahertz antireflection coating enabled by a subwavelength metallic mesh capped with a thin dielectric film

Li Huang [1*], Beibei Zeng [2], Chun-Chieh Chang [2] and Hou-Tong Chen [2*]
[1] Physics Department, Harbin Institute of Technology, Harbin, Heilongjiang 150001, China
[2] Center for Integrated Nanotechnologies, Los Alamos National Laboratory, Los Alamos, New Mexico 87545, USA
[*1] Email: lihuang2002@hit.edu.cn , [*2] Email: chenht@lanl.gov

(Received August 18, 2015)

Abstract: Metamaterials/metasurfaces have enabled unprecedented manipulation of electromagnetic waves. Here we present a new design of metasurface structure functioning as antireflection coatings. The structure consists of a subwavelength metallic mesh capped with a thin dielectric layer on top of a substrate. By tailoring the geometric parameters of the metallic mesh and the refractive index and thickness of the capping dielectric film, reflection from the substrate can be completely eliminated at a specific frequency. Compared to traditional methods such as coatings with single- or multi-layer dielectric films, the metasurface antireflection coatings are much thinner and the requirement of index matching is largely lifted. This approach is particularly suitable for antireflection coatings in the technically challenging terahertz frequency range and is also applicable in other frequency regimes.

Keywords: Metasurfaces, Antireflection coatings, Terahertz, Interference

doi: 10.11906/TST.1-9.2016.03.01

1. Introduction

Low absorption dielectric and semiconducting materials are very often used in terahertz (THz) photonic systems. For instance, high-resistivity silicon [1] is an excellent material widely used in THz applications, such as window, beam splitter, substrate of metamaterials, and lens for photoconductive transceiver. The large refractive index of silicon, however, results in approximately 32% Fresnel reflection loss under normal incidence at an air-silicon interface. The fringes caused by the Fabry-Pérot interference are also undesirable since they lower the spectral resolution and reduce the dynamic range of a THz spectroscopy system. Other typical crystalline materials for THz applications also have rather high refractive index values. Thus, antireflection coating becomes critical for performance improvement. In principle, antireflection coatings in the THz frequency range can be accomplished following the same approaches adopted in the optical regime, such as quarter-wave antireflection for narrow-band operation using a single-layer dielectric film with refractive index matched with the substrate, or broadband antireflection using multi-layer dielectric films with carefully arranged refractive indices and thicknesses [2].

However, in the THz frequency range, it is difficult to find low-loss dielectric materials with particular refractive index values and, at the same time, suitable for coating with tens of micrometer thickness [3, 4]. Ultrathin metallic films have been applied for THz antireflection, but suffered from undesirable high losses [5, 6]. Deep-subwavelength metal gratings were also exploited as THz antireflection coatings [7], by taking advantage of the diluted plasmonic response mimicking metal thin films, although it did not increase the transmission either. Bio-inspired subwavelength surface relief structures [8] with gradient-index have been applied to enable broadband antireflection in the THz frequency range [9-13], but they may be only applicable to certain materials or encounter challenging fabrications, and the structured surfaces may further pose difficulties in device integration.

New opportunities have arisen from the development of metamaterials [14, 15], which are a new class of artificially structured effective media exhibiting exotic properties and enabling emergent phenomena. One excellent example is metamaterial perfect absorbers where metamaterial structures are tailored to match the impedance of free space [16-18]. Following the similar strategy, metamaterial antireflection coatings have been successfully demonstrated a few years ago in the THz frequency range using a metal-dielectric-metal metamaterial structure [19, 20]. The most significant advantages of the metamaterial antireflection coatings include the ultra-thin thickness and no requirement of index matching for the dielectric spacer. This metamaterial antireflection approach was further simplified by removing one layer of metasurface structure, leaving only an array of metal resonators (metasurface) on top of a dielectric spacer deposited on a substrate [21]. Here we show another simplified metasurface structure consisting of a subwavelength metal mesh patterned on top of a substrate to be coated, with an additional layer of dielectric capping. Although subwavelength metallic mesh and the complementary structure were previously developed as interference filters in the far infrared [22, 23], we demonstrate that by appropriately tuning the geometric parameters and the thickness of the capping dielectric film, excellent antireflection function can be accomplished over a narrow bandwidth. The new design remains the same advantages as in the previous metamaterial structures while is much easier in fabrication.

2. Theoretical analysis

When an ultrathin subwavelength metallic structure is patterned at the boundary of two different dielectric media, it can be considered as a metasurface that modifies the reflection and transmission as well as their complex dispersion at the interface, which would be otherwise given by Fresnel equations. The reflection and transmission coefficients of the metasurface, schematically shown in Fig. 1(a), can be easily obtained through full-wave numerical simulations using commercially available packages such as CST Microwave Studio. In the case of multiple metasurfaces that are separated by thin dielectric spacers, multi-reflection occurs among the

metasurfaces, and the overall response is the superposition of the multiple reflections and transmissions, assuming near-field interactions between the neighboring metasurfaces are negligible. This is particularly true when the spacer thickness is larger than the metasurface near-field confinement, as verified by our previous works in metamaterial antireflection coatings and perfect absorbers [19, 24], where the weak near-field interactions can be considered as the first order perturbation [25].

Let's consider two metasurfaces that are separated by a thin dielectric spacer (refractive index n_2) on top of a substrate (refractive index n_3), as schematically shown in Fig. 1(b). For simplicity we assume normal incidence and lossless dielectric spacer and substrate. The total reflection and

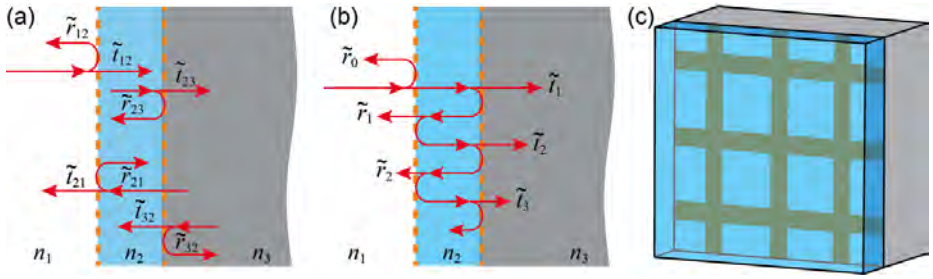

Fig. 1 Schematic of metamaterial antireflection coating structures. (a) Reflection and transmission at individual metasurfaces. (b) Multi-reflection between metasurfaces. (c) Metamaterial structure used in this work for antireflection coatings, consisting of a metal mesh on top of the substrate and capped by a thin dielectric film.

transmission coefficients are [19]:

$$\tilde{r} = \tilde{r}_{12} + \frac{\tilde{t}_{12}\tilde{r}_{23}\tilde{t}_{21}e^{j2\beta}}{1-\tilde{r}_{21}\tilde{r}_{23}e^{j2\beta}}, \tag{1}$$

$$\tilde{t} = \frac{\tilde{t}_{12}\tilde{t}_{23}e^{j\beta}}{1-\tilde{r}_{21}\tilde{r}_{23}e^{j2\beta}}, \tag{2}$$

where $\beta = -n_2 k_0 d$ is the propagation phase from one interface to the other, k_0 is the free space wave number, and d is the spacer thickness. Here we have used the convention of $e^{j\omega t}$ for the incident fields, consistent with the convention used in CST Microwave Studio. The first term in the right side of equation (1) is the direct reflection from the first interface, and the second term is the superposition of the multi-reflection.

The use of metasurface enables us to tune the desirable dispersion (both amplitude and phase) of the reflection and transmission coefficients through tailoring the metasurface structure. It becomes possible that the two terms in the right side of equation (1) destructively interfere and completely cancel out, resulting in the antireflection functionality. The transmission is consequently enhanced as compared to a bare substrate, as we demonstrated in our previous work

[19]. However, recent work has also shown that not both metasurfaces are required [21]; we can remove one metasurface as long as the refractive indices of the materials forming the interface have sufficiently large contrast. In the metamaterial antireflection coating structure used in this work, as shown in Fig. 1(c), we remove the metasurface at the air-spacer boundary, resulting in constant reflection and transmission coefficients. Then in equations (1) and (2), only $\tilde{r}_{23}$ and $\tilde{t}_{23}$ are dispersive, together with the frequency dependent propagation phase β. Through tailoring the mesh structure and spacer thickness, we show that the multi-reflection can be cancelled out and narrowband ideal antireflection can be accomplished.

3. Results and discussions

Using the metamaterial structure shown in Fig. 1(c), we first assume a fixed gold mesh structure with a period p = 62 μm and a line width w = 4 μm. Gold is simulated using the Drude model, where the plasma frequency $\omega_p = 2\pi \times 2181\, THz$ and the collision frequency $\upsilon_c = 6.5\ THz$. Both the substrate and the spacer have a refractive index $n_2 = n_3 = 3.42$, which is for silicon and close to values in other typical semiconductors (e.g., gallium arsenide) and dielectrics (e.g., sapphire and magnesium oxide) in the THz frequency range. The reflection and transmission coefficients at the air-spacer interface are then

$$\tilde{r}_{12} = \frac{n_1 - n_2}{n_1 + n_2} = -0.548; \quad \tilde{r}_{21} = \frac{n_2 - n_1}{n_2 + n_1} = 0.548$$

$$\tilde{t}_{12} = \frac{2n_2}{n_1 + n_2} = 1.548; \quad \tilde{t}_{21} = \frac{2n_1}{n_2 + n_1} = 0.452$$

where n_1 = 1 is for air. The complex reflection and transmission coefficients at the spacer-mesh-substrate interface are obtained from full-wave numerical simulations:

$$\tilde{r}_{23} = S_{22}; \quad \tilde{r}_{32} = S_{33}$$

$$\tilde{t}_{23} = \sqrt{n_3/n_2}S_{32} = S_{32}; \quad \tilde{t}_{32} = \sqrt{n_2/n_3}S_{23} = S_{23}$$

where the ports are named “2” and “3” at the spacer and substrate sides, respectively.

Inserting these values into equations (1) and (2), we semi-analytically obtain the overall reflection and transmission, as shown in Figs. 2(a) and (b), at various thicknesses of the capping dielectric film (i.e., varying the propagation phase β). Note that here we have defined the reflection and transmission as the square root of the power intensity (i.e., the same definition for S-parameters). It can be clearly seen that at all thicknesses the reflection (transmission) is

significantly suppressed (enhanced). The frequency of the reflection dip (transmission peak) decreases with the thickness of the capping film. Increasing the thickness starting from 15 μm, the reflection (transmission) first becomes lower (higher); when the thickness is near 25 μm, the reflection (transmission) approaches zero (unity) at around 0.6 *THz*; further increasing the thickness causes higher reflection and results in reduced antireflection performance. It is worth pointing out that around the ideal antireflection frequency (~0.6 *THz*) the reflection coefficient at the spacer-mesh-substrate is equal to that at air-spacer interface, which is consistent with the requirement pointed out in our previous metal-dielectric-metal metamaterial antireflection coating structure [19]. In contrast, in a quarter-wave antireflection coating it is accomplished only by index matching. The 25 μm thick capping film also provides an additional small propagation phase to satisfy the phase requirement for destructive interference of the multi-reflection, which has been largely provided by the reflection phase jump at both interfaces but would otherwise need the quarter-wave thickness of the coating material.

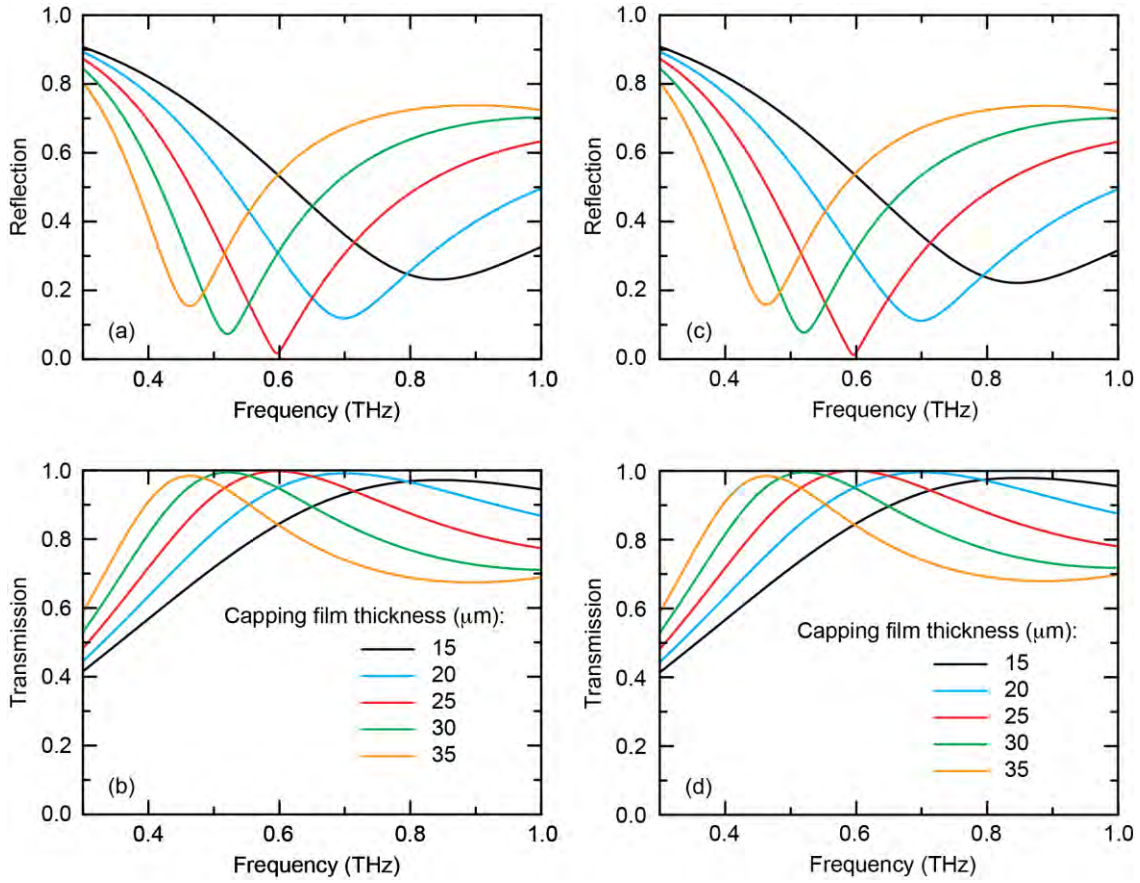

Fig. 2 Semi-analytically calculated reflection (a) and transmission (b) based on multi-reflection interference model, and full-wave simulated reflection (c) and transmission (d) at various thicknesses of the capping dielectric film.

Full-wave numerical simulations are performed to further validate this design concept of

metasurface antireflection coatings. In this case, both interfaces are present within the unit cell, where any interactions (e.g., due to the evanescence fields) have been taken into account. The reflection and transmission are plotted in Figs. 2(c) and (d) as functions of the thickness of the capping dielectric film. Compared with the reflection and transmission (shown in Figs. 2(a) and (b)) calculated through the semi-analytical approach, we observe an excellent agreement between the results obtained using the two different approaches, demonstrating that the two interfaces can be treated separately and the near-field interaction is negligible. It also validates that high-performance antireflection coatings can be accomplished using a single layer metasurface capped with a dielectric film of appropriate thickness. The near-unity transmission also manifests that the losses caused by the gold mesh are negligible in the THz frequency range.

As pointed out, one of the advantages of metasurface antireflection coating is no requirement of index matching for the coating materials. In order to illustrate this, we change the refractive index of the capping dielectric film to n_2 = 2.45, while keeping the mesh structure the same as before. The reflection spectra obtained through full-wave numerical simulations are shown in Fig. 3 at various thicknesses of the capping film. It is clearly shown that, ideal antireflection is again accomplished when the thickness is correctly chosen. The antireflection frequency of 0.9 *THz* is, however, different as compared with the previous case where the capping film refractive index is n_2 = 3.42. This is reasonable as the dispersion of the mesh and the propagation phase within the capping film change with the refractive index. Note that the thickness of ~25 μm for ideal antireflection performance, nearly the same as the previous case, is only a coincidence.

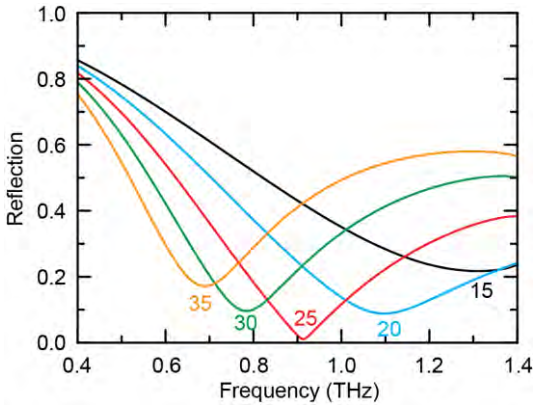

Fig. 3 Reflection at various thicknesses (unit: μm) obtained using full-wave numerical simulations with the capping film refractive index n_2 = 2.45.

By tailoring the geometric parameters of the mesh structure, and the refractive index and thickness of the capping dielectric film, the metasurface antireflection coating can operate at any relevant frequency in the THz and infrared frequency regimes. The only restrictions are (i) the

metallic losses that may limit the applications at near-infrared and visible frequencies and (ii) the availability of low-loss dielectric materials that are suitable for coating. In the THz frequency range, one may laminate the device layer of a silicon-on-insulator wafer as the capping dielectric film, for instance, using a thin layer of photoresist as the adhesion. The handle layer is then etched away with the insulator layer (silicon dioxide) as the etching stop and consequently removed. In the infrared frequency range, one may directly deposit amorphous silicon as the capping dielectric film. The experimental demonstration of this metasurface antireflection coating concept will be presented in a separated publication.

4. Conclusion

We have proposed a new design of metasurface antireflection coating consisting of a single-layer metasurface (subwavelength metallic mesh) capped with a thin dielectric film. The antireflection coating is based on the destructive interference of the multi-reflection between the air-dielectric interface and the dielectric-mesh-substrate interface. By tuning the geometric parameters of the mesh and the thickness of the capping dielectric film, the reflection from the substrate is minimized approaching zero and the transmission is enhanced to near-unity. The metasurface antireflection coating does not require index matching of the dielectric film to the substrate, and the simplified metasurface structure is easy to fabricate. It is numerically demonstrated in the THz frequency range and is expected to operate in the other frequency regimes where the metallic losses are negligible.

L. Huang acknowledges support in part from Fundamental Research Funds for the Central Universities and Program for Innovation Research of Science in Harbin Institute of Technology (PIRS OF HIT) under Grant No. T201408. We acknowledge partial support from the Los Alamos National Laboratory Laboratory Directed Research and Development program. This work was performed, in part, at the Center for Integrated Nanotechnologies, an Office of Science User Facility operated for the U.S. Department of Energy (DOE) Office of Science. Los Alamos National Laboratory, an affirmative action equal opportunity employer, is operated by Los Alamos National Security, LLC, for the National Nuclear Security Administration of the U.S. Department of Energy under contract DE-AC52-06NA25396.

References

[1] D. Grischkowsky, S. Keiding, M. van Exter, et al.. “Far-infrared time-domain spectroscopy with terahertz beams of dielectrics and semiconductors”. *J. Opt. Soc. Am. B* 7, 2006-2015 (1990).

[2] M. Born and E. Wolf. *Principles of Optics* (Pergamon, 1980).

[3] I. Hosako. "Antireflection coating formed by plasma-enhanced chemical-vapor deposition for terahertz-frequency germanium optics". *Appl. Opt.* 42, 4045-4048 (2003).

[4] K. Kawase and N. Hiromoto. "Terahertz-wave antireflection coating on Ge and GaAs with fused quartz". *Appl. Opt.* 37, 1862-1866 (1998).

[5] J. Krödl, J. Darmo, and K. Unterrainer. "Metallic wave-impedance matching layers for broadband terahertz optical systems". *Opt. Express* 15, 6552-6560 (2007).

[6] A. Thoman, A. Kern, H. Helm, et al.. "Nanostructured gold films as broadband terahertz antireflection coatings". *Phys. Rev. B* 77, 195405 (2008).

[7] L. Ding, Q. Y. S. Wu, J. F. Song, et al.. "Perfect broadband terahertz antireflection by deep-subwavelength, thin, lamellar metallic gratings". *Adv. Opt. Mater.* 1, 910-914 (2013).

[8] J. Cai and L. Qi. "Recent advances in antireflective surfaces based on nanostructure arrays". *Mater. Horiz.* 2, 37-53 (2015).

[9] C. Brückner, T. Käsebier, B. Pradarutti, et al.. "Broadband antireflective structures applied to high resistive float zone silicon in the THz spectral range". *Opt. Express* 17, 3063-3077 (2009).

[10] Y. W. Chen, P. Y. Han, and X.-C. Zhang. "Tunable broadband antireflection structures for silicon at terahertz frequency". *Appl. Phys. Lett.* 94, 041106 (2009).

[11] Y. W. Chen, P. Han, X.-C. Zhang, et al.. "Three-dimensional inverted photonic grating with engineerable refractive indices for broadband antireflection of terahertz waves". *Opt. Lett.* 35, 3159-3161 (2010).

[12] S.-I. Kuroo, S. Oyama, K. Shiraishi, et al.. "Reduction of light reflection at silicon-plate surfaces by means of subwavelength gratings in terahertz region". *Appl. Opt.* 49, 2806-2812 (2010).

[13] R. Datta, C. D. Munson, M. D. Niemack, et al.. "Large-aperture wide-bandwidth antireflection-coated silicon lenses for millimeter wavelengths". *Appl. Opt.* 52, 8747-8758 (2013).

[14] D. R. Smith, W. J. Padilla, D. C. Vier, et al.. "Composite medium with simultaneously negative permeability and permittivity". *Phys. Rev. Lett.* 84, 4184-4187 (2000).

[15] V. M. Shalaev. "Optical negative-index metamaterials". *Nat. Photon.* 1, 41-48 (2007).

[16] C. M. Watts, X. L. Liu, and W. J. Padilla. "Metamaterial electromagnetic wave absorbers". *Adv. Mater.* 24, Op98-Op120 (2012).

[17] L. Huang and H.-T. Chen. "A Brief review on terahertz metamaterial perfect absorbers". *THz Sci. Technol.* 6, 26-39 (2013).

[18] N. I. Landy, S. Sajuyigbe, J. J. Mock, et al.. "Perfect metamaterial absorber". *Phys. Rev. Lett.* 100, 207402 (2008).

[19] H.-T. Chen, J. F. Zhou, J. F. O'Hara, et al.. "Antireflection coating using metamaterials and identification of its

mechanism". *Phys. Rev. Lett.* 105, 073901 (2010).

[20] H.-T. Chen, J. Zhou, J. F. O'Hara, et al.. "A numerical investigation of metamaterial antireflection coatings". *THz Sci. Technol.* 3, 66-73 (2010).

[21] B. Y. Zhang, J. Hendrickson, N. Nader, et al.. "Metasurface optical antireflection coating". *Appl. Phys. Lett.* 105, 241113 (2014).

[22] R. Ulrich. "Far-infrared properties of metallic mesh and its complementary structure". *Infrared Phys.* 7, 37-55 (1967).

[23] R. Ulrich. "Interference Filters for the Far Infrared". *Appl. Opt.* 7, 1987-1996 (1968).

[24] H.-T. Chen. "Interference theory of metamaterial perfect absorbers". *Opt. Express* 20, 7165-7172 (2012).

[25] L. Huang, D. Roy Chowdhury, S. Ramani, et al.. "Impact of resonator geometry and its coupling with ground plane on ultrathin metamaterial perfect absorbers". *Appl. Phys. Lett.* 101, 101102 (2012).